This is a preprint, the final version is subject to change, of the American Mineralogist (MSA)
Cite as Authors (Year) Title. American Mineralogist, in press.
(DOI will not work until issue is live.) DOI: http://dx.doi.org/10.2138/am.2013.4310

Crystal structure and chemistry of skarn-associated bismuthian vesuvianite

Ulf Hålenius[1], Ferdinando Bosi[2] and Kjell Gatedal[3]

[1]Department of Mineralogy, Swedish Museum of Natural History, Box 50007, SE-104 05 Stockholm, Sweden

[2]Dipartimento di Scienze della Terra, Sapienza Università di Roma, Piazzale Aldo Moro 5, I-00185 Roma, Italy

[3]Nordmark Mining Museum, SE-683 93 Nordmark, Sweden

ABSTRACT

Due to its strong chalcophile character and the influence of its s^2 lone pair electrons on the crystal structure trivalent bismuth is extremely rare in silicate minerals, with Bi-contents in common silicates typically below 1 ppm. In the present paper we report on an exceptionally Bi-rich variety of the rock-forming mineral vesuvianite with up to ca. 20 wt% Bi_2O_3, occasionally in combination with enhanced Pb contents up to ca. 5 wt% PbO. The mineral occurs as small ($\leq$ 300 μm) idiomorphic, black crystals in a sulfide-free silicate skarn in the Långban Mn-Fe deposit, central Sweden. The major skarn minerals comprise Ba-rich potassium feldspar, albitic plagioclase and Pb-rich scapolite and phlogopite, while Pb-rich epidote, vesuvianite and calcic garnets are minor phases. The vesuvianite grains are intensely zoned displaying Bi-rich cores surrounded by thinner Bi-poor rims. Although generally high in bismuth, the crystal cores invariably show oscillatory zoning. In addition to high Bi- and Pb-contents, the crystals are occasionally enriched in copper, cerium, antimony and arsenic, thus reflecting the complex chemistry and evolution of the Långban mineralization.

Chemical analyses demonstrate a strong negative correlation between Ca and Bi, hence confirming that Bi replaces Ca at X-sites of the vesuvianite structure. Concentrations of Si and Al are lower, while Fe and Ti contents are somewhat enhanced in the Bi-rich cores. Maximum Bi and Pb contents analyzed in the present vesuvianite crystals correspond to 3.19

and 0.87 atoms per formula unit, respectively. This exceeds by far previous reports in the literature. X-ray single-crystal diffraction studies of a crystal splinter with intermediate Bi-content (1.08 apfu) show that the space group *P4/nnc* is the most appropriate to describe the crystal structure; the refinement converged to an *R*1 index of 0.0493. The recorded unit-cell parameters, a = 15.7018(6) Å, c = 11.8648(6) Å and V = 2925.2(2) Å^3, are to our knowledge the largest ones observed so far for *P4/nnc* vesuvianite. Bismuth was demonstrated to order at the X3´(Bi) site that is only 0.46 Å distant from the nearest X3(Ca) site. Consequently, the X3 and X3´ sites cannot be simultaneously fully occupied.

INTRODUCTION

The ionic radii of six- to eight-coordinated Bi^{3+} (1.03-1.17 Å) are very similar to those of Na^{+} (1.02-1.18 Å), Ca^{2+} (1.00-1.12 Å) and trivalent cations of the light rare earth elements, as, e.g., Ce^{3+} (1.01-1.14Å) (Shannon 1976). This suggests that cases of Bi^{3+} substitution in rock-forming Na- and/or Ca-silicates shouldn't be uncommon. However, Bi-contents are generally very low (< 1ppm) in silicate minerals and only two extremely rare silicate minerals with nominal Bi-contents are known; eulytine ($Bi_4(SiO_4)_3$) and bismutoferrite ($Fe^{3+}{}_2Bi(SiO_4)_2(OH)$). In contrast, Bi-contents may reach high levels in common sulfide minerals and a large number of Bi-sulfide mineral species are known. Main reasons for this are the affinity for Bi^{3+} to form covalent bonds to sulfur (chalcophile character) and the $6s^2$ lone pair electronic configuration of Bi^{3+} that prefers highly unsymmetrical coordination in oxygen-based structures. However, the stereochemical effects of the lone pair configuration weaken with increasing coordination number of the Bi-centered polyhedra (Galy et al. 1975) and this creates possibilities for Bi-incorporation in certain silicate structures when formed in environments poor in sulphur. In the present paper we

52 report on the crystal chemistry of an extremely Bi-rich vesuvianite that represents an
53 exceptional example of Bi^{3+} substitution in a rock-forming silicate mineral.

54 The simplified formula of boron-free vesuvianite can be written as $X_{19}Y_{13}Z_{18}O_{69}W_{10}$,
55 where X represents four independent [7]- to [9]-coordinated sites, Y represents one [5]-
56 coordinated (Y1) and two independent [6]-coordinated sites (Y2 and Y3), Z denotes three
57 distinct [4]-coordinated sites and W represents the sites (O10 and O11) occupied by
58 monovalent and divalent anions such as (OH), F and O (Groat et al. 1992a,b). Vesuvianites
59 with empty T sites, $^{[4]}$T1 and $^{[3]}$T2, have 10 W-sites in the structural formula, whereas
60 vesuvianites with [3]-coordinated B at T2 have 11 W-sites due to the substitution $^{T2}B + 2^{W}O$
61 $\rightarrow {}^{T2}\square + {}^{W}(OH)$ (Groat et al. 1996). The general formula for vesuvianite group minerals may
62 therefore be formalized as $X_{18}X'Y_{12}Y'T_5{}^{O}Z_{10}{}^{D}Z_8O_{68}(W)_{11}$, where "O" and "D" denote ortho-
63 and disilicate groups and W represents sites occupied by atoms not bonded to cations at the Z
64 sites (Gnos and Armbruster 2006). The X' and Y' sites form polar strings along the fourfold
65 axis and the schemes of order determine the symmetry of the structure, with the possible
66 space groups *P4/nnc*, *P4/n* and *P4nc* (Armbruster and Gnos 2000a). Generally, vesuvianite
67 formed at higher temperatures, above ca. 500 °C, crystallizes in space group *P4/nnc* (Gnos
68 and Armbruster 2006). In addition, partial Al occupancy at the T1 site seems to cause rod
69 disorder resulting in *P4/nnc* symmetry (Gnos and Armbruster 2006).

70 Chemically, vesuvianite shows a wide range of compositions. The Z-sites are
71 normally occupied by Si^{4+}, but Si-deficient vesuvianites with high degrees of hydrogarnet-like
72 substitution, $(O_4H_4)^{4-}$ for $(SiO_4)^{4-}$, are also known (Armbruster and Gnos 2000b, Galuskin et
73 al. 2003). A large number of different cations have been shown to occupy the Y-sites of the
74 vesuvianite structure. Magnesium, Al, Ti^{4+}, Mn^{2+}, Mn^{3+}, Fe^{2+}, Fe^{3+} and Cu^{2+} are common Y-
75 site cations, while Cr^{3+} and Zn^{2+} are found at lower levels (e.g., Groat et al. 1992a and
76 references therein). Groat et al. (1994a) demonstrated that additional "Y-group" cations may

occupy the normally vacant T1 site of the vesuvianite structure. In addition, B^{3+} occupies the normally vacant T2 site in boron-rich vesuvianites (Groat et al. 1994b, 1996). The most common cations at the structural X-sites are Ca and Na, but low to intermediate contents of a large number of additional cations, such as, e.g., REE (Fitzgerald et al. 1987) and U and Th (Himmelberg and Miller 1980) have been reported. High contents of Sb (21.2 wt% Sb_2O_3 corresponding to ca. 4.9 Sb per formula unit) have been reported in vesuvianites from the Hemlo deposit (Pan and Fleet 1992) and notably, an occurrence of Bi-bearing vesuvianites with up to 3.1 wt% Bi_2O_3 (0.41 Bi per formula unit) was recently described from Långban, Sweden (Groat and Evans 2012). In the present study we report structural and chemical data for a Bi-rich variety of vesuvianite with ~7 times higher Bi-contents, and Pb-contents up to 3 times higher than in earlier literature reports.

In spite of the large chemical and structural diversity, the number of approved species belonging to the vesuvianite group is very limited: vesuvianite $Ca_{19}Mg_2Al_{11}Si_{18}O_{68}(O)(OH,F)_9$, wiluite $Ca_{19}Mg_6Al_7B_5Si_{18}O_{68}(O)_{11}$ (Groat et al. 1998), manganvesuvianite $Ca_{19}Mn^{3+}(Al,Mn^{3+},Fe^{3+})_{10}(Mg,Mn^{2+})_2Si_{18}(O)O_{68}(OH)_9$ (Armbruster et al. 2002), and fluorvesuvianite $Ca_{19}(Al,Mg,Fe^{2+})_{13}Si_{18}O_{68}O(F,OH)_9$ (Britvin et al. 2003). In analogy with the definition of manganvesuvianite, which is based on the dominant cation at the Y1-site being Mn^{3+}, it is evident that vesuvianite with Cu^{2+} as the dominant cation at Y1 (Fitzgerald et al. 1986) is also a distinct species of the vesuvianite mineral group. The potential for the existence of several additional vesuvianite group species is very high. For example, data published by Pan and Fleet (1992) and the data presented in this study highlight the possible occurrence of antimonian and bismuthian end members.

GEOLOGICAL SETTING

Ores and their Palaeoproterozoic host rocks in the Bergslagen region of south-central Sweden formed within a mostly shallow submarine, felsic caldera province, situated in a back arc setting in the close vicinity of a continental margin (Allen et al. 1996). A majority of the mineralisations are believed to have formed through hydrothermal processes within this environment during felsic volcanism (Allen et al. 1996). Skarn-hosted deposits dominated by magnetite, and quartz-banded ores dominated by hematite represent the major oxide deposits in the district. In the Fe-Mn oxide deposits of Långban-type, the two oxide ore types occur in spatial proximity, but are chemically well separated.

The Långban deposit (59.86°N, 14.27°E) comprises stratabound ore lenses rich in Fe and Mn oxides, with associated skarn bodies and mineralised veins and fissures hosted by metamorphosed carbonates and siliceous volcanics of early Proterozoic age (~1.85 Ga) and it is generally considered to be of syngenetic, submarine volcanic-exhalative origin (Boström et al. 1979; Holtstam and Mansfeld 2001; Jonsson 2004). Together with related deposits in west-central Sweden, it is characterised by enhanced contents of As, Ba, Be, Pb and Sb. Fluids derived from younger granite intrusions subsequently introduced additional chemical components such as Be, F, Sn and W (e.g., Holtstam and Mansfeld 2001).

The evolution of the deposit has been subdivided into four separate major stages (Magnusson 1930; Jonsson 2004). Initial formation of "primary" minerals, including early carbonates and ore mineral progenitors was followed by a ca. 1.87-1.80 Ga regional (Svecokarelian) metamorphism of the Bergslagen region (e.g., Welin 1992; Andersson 1997; Stephens et al. 2009, and references therein). In the Långban area, peak regional metamorphic conditions are estimated to have reached ca. 3-4 kbar and 550-600 °C (e.g., Grew et al. 1994; Christy and Gatedal 2005), i.e., amphibolite facies conditions. During this stage the majority of skarn (*sensu lato*) minerals and veins were formed. Subsequently, formation of vein mineral assemblages related to a stage of waning metamorphism were foloowed by late stage

mineral veining at lower temperatures ranging from 180 to 300 °C (Jonsson and Broman 2002).

The Långban deposit is famous for its mineral diversity (e.g., Flink 1923; Magnusson 1930; Moore 1970; Holtstam and Langhof 1999). About 300 mineral species have been documented and more than 70 new mineral species have been discovered and described from this locality. The deposit is famous not just for new species, but also for unusual chemical compositions of common minerals (Christy and Gatedal 2005).

SAMPLES AND EXPERIMENTAL

Samples

The Långban mine is inaccessible today and the present samples were collected from the dump near the New Shaft (Nya Schaktet) at Långban. The studied samples comprise five chips of skarn rocks that are mainly composed of K-feldspar, plagioclase, scapolite, epidote and phlogopite with garnet and vesuvianite as minor minerals. Accessory minerals are calcite, titanite, muscovite and zircon. Energy dispersive X-ray analyses on carbon-coated polished sections of the samples using a Hitachi S4300 scanning electron microscope (SEM) equipped with a solid state Si(Li) detector were applied to explore the chemical character of the main and minor phases accompanying vesuvianite. The SEM was operated at an acceleration voltage of 20 kV and a beam current of 10 nA using an electron beam diameter of ca. 1 μm. The energy dispersive X-ray spectra (EDS) were recorded and evaluated using the INCA software package (Oxford Instruments). The results of this reconnaissance demonstrated that K-feldspar is rich in barium, plagioclase is albitic in composition and scapolite (intermediate between meionite and amrialite) as well as epidote are Pb-rich. Garnet compositions vary along the grossular-andradite join with only limited spessartine component present. The

mineral composition of the present vesuvianite-bearing skarn as well as the chemical signatures of its major and minor minerals show many features in common with those of the vesuvianite-free Långban skarn assemblages described by Christy and Gatedal (2005) and consequently the present skarn assemblage is considered to have formed at comparable conditions, i.e., during the peak metamorphic event at temperatures exceeding 500 °C. The mineral assemblage of the high-temperature skarn hosting the present extremely Bi-rich vesuvianite contrasts strongly with the hausmannite ore association that hosts the Bi-bearing vesuvianite described from the same locality by Groat and Evans (2012). The black color of the present Bi-rich vesuvianite crystals is also in contrast to the red color reported for the Bi-bearing vesuvianite by Groat and Evans (2012).

The present vesuvianite crystals frequently display micro-fractures and they are without exception highly brittle. Consequently, only crystal splinters could be extracted for single-crystal structure studies. X-ray diffraction studies of several of these crystal fragments yielded poor quality data and subsequent refinements of the data did not converge. This was also the case for fragments of the most Bi-rich crystal cores. However, successful structure refinements were obtained on fragments with intermediate compositions showing more than twice the Bi contents earlier reported.

Chemical analyses

Electron microprobe analyses (EMPA) by wavelength dispersive spectroscopy (WDS) were obtained with a Cameca SX50 instrument at the University of Uppsala operating at an accelerating potential of 20 kV and a sample current of 15 nA. Standards used comprised wollastonite (Si and Ca), vanadinite (Pb), Al_2O_3 (Al), Bi_2S_3 (Bi), $CePO_4$ (Ce), Cu metal (Cu), Fe_2O_3 (Fe), MgO (Mg), $MnTiO_3$ (Mn and Ti), Sb_2S_3 (Sb) and ZnS (Zn). Chlorine and fluorine were searched for by WDS-scans but could not be detected and consequently

these elements were not analyzed for due to concentrations below their detection limits (0.2 and 0.05 wt%, respectively). The PAP matrix correction procedure (Pouchou and Pichoir 1991) was applied to the obtained raw data.

Single-crystal X-ray structure refinement

X-ray diffraction measurements were performed at the Earth Sciences Department, Sapienza University of Rome, with a Bruker KAPPA APEX-II single-crystal diffractometer, equipped with CCD area detector (6.2 × 6.2 cm^2 active detection area, 512 × 512 pixels) and a graphite crystal monochromator, using Mo*K*α radiation from a fine-focus sealed X-ray tube. The sample-to-detector distance was 4 cm. A total of 3304 exposures (step = 0.2°, time/step = 20 s) covering a full reciprocal sphere were collected. The orientation of the crystal lattice was determined from more than 500 strong reflections ($I > 100\ \sigma_I$) evenly distributed in the reciprocal space, and used for subsequent integration of all recorded intensities. Final unit-cell parameters were refined by using Bruker AXS SAINT program from ca. 4439 recorded reflections with $I > 10\ \sigma_I$ in the range $7° < 2\theta < 61°$. The intensity data were processed and corrected for Lorentz, polarization and background effects with the APEX2 software program of Bruker AXS. The data were corrected for absorption using a multi-scan method (SADABS). The absorption correction led to a significant improvement in R_{int}.

In agreement with the indications of the systematic absence statistics, the *P*4/*nnc* symmetry was used for the final structure refinement. The recorded data for the crystal showed only one systematic absence violation for *P*4/*nnc*. Groat and Evans (2012) also found this space group in successful structure refinements of two Bi-bearing vesuvianites. The fact that the space group *P*4/*nnc* is the most appropriate to describe the structure of the present sample is also shown by the negative result of two tests suggested by Armbruster and Gnos (2000a) for the possible occurrence of space group *P*4*nc* or *P*4/*c* in alternative to *P*4/*nnc*: (1)

no distribution with $F_o^2 > F_c^2$ in the list of most disagreeable reflections was observed in our refinement; (2) the K values, where K = mean(F_o^2)/mean(F_c^2), were always less than 1.4, showing that our structural model is correct. Finally, petrological observations, as detailed above, show that the present vesuvianite occurs in a high-temperature skarn assemblage, which is consistent with its space group being *P*4/*nnc* (Gnos and Armbruster 2006).

Structure refinement (SREF) was carried out with the SHELXL-97 program (Sheldrick 2008). Starting coordinates were taken from Groat and Evans (2012). Variable parameters were: scale factor, extinction coefficient, atom coordinates, site-scattering values expressed as mean atomic number (m.a.n.) and atom displacement parameters. To obtain the best values of statistical indices (*R*1 and w*R*2) all atomic sites were modeled by using neutral scattering curves. In detail, all the anion sites (O1-O11) were modeled by using oxygen scattering factor and with a fixed occupancy of 1, because refinement with unconstrained occupancies showed no significant deviations from this value. The X1 and X2 sites were modeled using the Ca scattering factor with fixed occupancy of $Ca_{1.00}$. The X3 site X3' sites were modeled by Ca and Bi, respectively. The X4 site was modeled considering the presence of Ca and Ce. The Y1 site was modeled considering Mn and Mg. The Y2 site was modeled using Al, and Y3 considering Al and Fe. The Z1 and Z2 site were modeled by using Si with unconstrained occupancies, while Z3 was modeled by Si with a fixed occupancy of $Si_{1.00}$. The T1 site, found in the residual electron density, was modeled by Al. Table 2 summarizes crystal data, data collection information and refinement details. Table 3 provides the refined atom coordinates, equivalent and isotropic displacement parameters, and m.a.n.. Table 4 (on deposit) reports the anisotropic displacement parameters. Table 5 lists selected bond lengths, and Table 6 displays bond valence sums (calculated from Brown and Altermatt 1985) incident at the cation sites and the respective mean formal valences.

RESULTS AND DISCUSSION

Vesuvianite composition

The vesuvianite grains are strongly zoned, displaying Bi-rich cores surrounded by thinner Bi-poor rims (Fig. 1 and Table 1). Although generally high in Bi, the crystal cores invariably show oscillatory zoning. Concentrations of Si and Al are lower while Fe and Ti contents are somewhat enhanced in the Bi-rich cores (Fig. 2). In addition to high Bi contents, some crystals display zones with high Pb contents (up to 0.87 apfu) and some crystals occasionally show zones enriched in Cu, Ce, As and Sb, thus reflecting the complex chemistry and evolution of the Långban mineralization. The maximum Bi content recorded in the analyzed specimens is 20.42 wt%, corresponding to Bi^{3+} = 3.19 apfu (Table 1 and Fig. 2). This exceeds the Bi concentration in vesuvianite reported by Groat and Evans (2012) by ~7 times. Apart from considerably higher Bi contents and the occurrence in a different mineral association, our vesuvianite crystals show distinctly lower Mn contents (≤ 0.62 apfu) as compared to those reported (Mn 1.43-1.76 apfu) by Groat and Evans (2012). The Bi content of our crystals shows a strong negative correlation (r^2 = 0.989) with other cations (mostly Ca and Pb and Ce to a lesser degree) located at the X sites (Fig. 3), which demonstrates that Bi proxies for Ca at the X-sites.

Single crystal structure refinement

Although the crystallographic *R*-indices appear to be relative large in the present Bi-rich vesuvianite (Table 2), they are comparable to those obtained by Groat and Evans (2012) for two Bi-bearing vesuvianites. However, it is important to stress the fact that the quality of a structural model should be assessed, for example, by the standard uncertainty of the bond distances, which should be less than 0.006 Å for non-hydrogen atoms (Giacovazzo et al.

2002), rather than only by the *R*-indices. The refinement of the present sample meets such criteria. The causes of the relative large displacement parameter values (e.g., Table 3) can be ascribed to: (1) the typical static positional disorder involving both cations and anions of vesuvianite; (2) the poor quality of the crystal; (3) the poor absorption correction, presumably due to the shape of the fragment used for the X-ray diffraction collection (0.02 mm-thick flake). All these negative aspects tend to affect the displacement parameters, but fortunately the atomic positions are much less perturbed. It is noteworthy that structure refinements using split site models did not result in any improvements.

Site occupancies

The X1 site. The X1-m.a.n. was constrained to 20 as no significant deviation from the full occupancy of Ca^{2+} was noted during the refinement process. Both the mean bond-distance <X1-O>, 2.439 Å, and the bond valence sum (BVS) at X1, 2.31 valence units (vu), are consistent with those reported by Groat et al. (1992a,b) for a boron-free vesuvianite (sample V12) having an X1 site completely occupied by Ca.

The X2 site. The X2-m.a.n. was constrained to 20 as no significant deviation from the full occupancy of Ca^{2+} was noted during the refinement process. <X1-O> = 2.491 Å and X2-BVS = 2.16 vu are consistent with a complete occupancy of Ca^{2+} at X2.

The X3 site. In accordance with Groat and Evans (2012), two distinct X3 sites were found during the structure refinement of the present Bi-rich vesuvianite: X3 (≡ Ca) and X3' (≡ Bi). The sum of refined site-scattering values of (X3 + X3') converged to a site occupancy of 0.935, i.e., less than 1.00. This means that cation vacancies occur at these sites as a function of the occurrence of cations at the T1 structural site (see below). The refined site occupancy of X3 converged to 0.811 and X3-m.a.n. to 16.2(1). The X3 site is usually considered as [8]-fold coordinated, however in [9]-fold coordination (that is, including a long

277 X3-O6 distance), the X3-BVS value increases from 1.77 vu to 1.85 vu. Obviously, the latter
278 value is closer to ideal value of 2.00 expected for Ca^{2+} (Tables 5 and 6). It should be noted
279 that whether in [8]- or in [9]-fold coordination, the X3-centered polyhedron is the largest
280 polyhedron of the present structure (Table 5). As for the X3' site, the refined site occupancy
281 equals 0.124, the m.a.n. converged to 10.3(1) and <X3'-O> to 2.529 Å. This information
282 along with the BVS incident at X3' (3.09 vu) show that this site can be considered as
283 exclusively occupied by Bi^{3+}. Groat and Evans (2012) named the Bi site XBi, we choose to
284 label it as X3' to underline its direct relationship to the X3 site of the vesuvianite structure
285 (Fig. 4a and Fig. 4b). It should be noted that because the X3' site is only 0.463(2) Å apart
286 from the X3 site, X3' cannot be occupied when the directly adjacent X3 site is occupied. This
287 X3′-X3 distance compares very well with those (0.41(2) and 0.44(2) Å) reported by Groat
288 and Evans (2012),

289 **The X4 site.** The observed X4-m.a.n., 11.6(1), and X4-BVS, 2.22 vu, are significant
290 larger than 10 and 2.00 (respectively) that would be expected for a half-occupancy of the X4
291 site by Ca^{2+}. This suggests that small amounts of trivalent cations such as Ce^{3+} may occur at
292 the X4 site. As reported by Groat et al. (1992a) and Allen and Burnham (1992) the X4 site of
293 vesuvianite is only half-occupied due to the occurrence of the short X4-X4 distance in the
294 structure (~2.57 Å in our sample), which implies occupancy of only one of two X4
295 crystallographic sites per formula unit. Comparable arguments, strictly linked to the occupied
296 X4-site, explain the half-occupancy of the Y1 sites. The separation of Y1-X4 is too small
297 (~1.11 Å for our sample) for the simultaneous occupancy of adjacent Y1 and X4 sites.

298 **The Y1 site.** The refined Y1-m.a.n. converged to 10.9(3) and <Y1-O> to 2.095 Å; the
299 experimental BVS at Y1 is equal to 1.95 vu. As this site is usually half-occupied (see
300 comment above), the m.a.n. would be 12.5 if only Mn would occupy Y1. Consequently,
301 significant amounts of lighter divalent atoms such as Mg^{2+} (Z = 12) must occur at Y1.

The Y2 site. The refined Y2-m.a.n. converged to 13.5(2) and <Y2-O> to 1.912 Å; the experimental BVS at Y2 is equal to 3.13 vu. These values suggest that Y2 is dominated by trivalent cations such as Al (Z = 13), but atoms with Z > 13 (as, e.g., Ti and Fe) must also occur. In general, the vesuvianite Y2 site is completely occupied by Al (e.g., Groat and Evans 2012), which underscores the unusual character of the present specimen.

The Y3 site. The refined Y3-m.a.n. converged to 15.0(1) and <Y3-O> to 1.988 Å; the experimental BVS at Y3 is equal to 2.68 vu. These values suggest that Al is the dominant cation at Y3, but atoms with Z > 13 (as, e.g., Ti and Fe) must also occur.

The T1 site. The refined T1-m.a.n. converged to 1.43(2) and <T1-O> to 1.816 Å; the BVS incident at T1 is 2.82 vu. This suggests presence of Al^{3+} at T1. The refined site occupancy of T1 (0.11) is consistent with the occurrence of vacancies at the X3 site (Groat et al. 1994a; Groat and Evans 2012). In fact, the combined occupancies of the X3, X3'and T1 sites (= 1.04) is, within experimental uncertainty, close to 1.00.

The Z1 site. The refined Z1-m.a.n. converged to 13.1(2) and <Z1-O> to 1.643 Å; the BVS at Z1 is 3.80 vu. Both the m.a.n. and the BVS values suggest that this site might not be fully occupied by Si^{4+} (Z = 14), but lighter elements such as Al or vacancies (up to 0.13 apfu) could be present.

The Z2 site. The refined Z2-m.a.n. converged to 13.0(1) and <Z2-O> = 1.649 Å, the BVS at Z2 is 3.74 vu. Similar to Z1, both the m.a.n. and the BVS values suggest that Al or vacancies (up to 0.54 apfu) could occur at Z2. In this regard, however, it is worthy to note that Groat et al. (1992a) and Groat and Evans (2012) reported values of BVS at Z1 and Z2 of ~3.8 vu and <Z1-O> and <Z2-O> of ~1.64 Å for boron-free vesuvianites with Z1 and Z2 fully occupied by Si.

The Z3 site. The Z3-m.a.n. was refined to 14, and <Z3-O> converged to 1.634 Å; the BVS incident at Z3 is 3.90 vu. These values indicate that Z3 is fully occupied by Si^{4+}.

Structural formula

The SREF-derived composition of the fragment used for the X-ray single-crystal diffraction data collection agrees very well with the microprobe data (analysis 740:X1SREF in Table 1). In particular, there is a very good match between the Bi content derived from SREF and EMPA (about 1.00 apfu and 1.08 apfu, respectively) as well as between the concentrations of Al at T1 derived from SREF and the excess Y-group cations derived from EMPA (about 0.11 apfu). Such cation excesses can be ascribed to Al (Groat et al. 1994a). Also important, in this respect, is the fact that the analysis 740:X1SREF is free of As, which , is expected to occupy the T1 site (Groat and Evans 2012).

Except for the ordering of Cu^{2+} at Y1 (Fitzgerald et al. 1986), there exists a number of alternative cation occupancy schemes for Y1, Y2 and Y3 sites in vesuvianite. Consequently, the cation distributions at these sites were calculated by a least-squares program in which the residual between calculated and observed m.a.n as well as between the BVS at Y1, Y2 and Y3 and the respective mean formal valence were minimized. Such an approach is very similar to that used to obtain cation distributions in spinel and tourmaline (e.g., Bosi et al. 2010; Bosi et al. 2010).

The resulting structural formula is:

$$^{X1}(Ca)_{\Sigma 2.00}{}^{X2}(Ca)_{\Sigma 8.00}{}^{X3}(Ca_{6.70}Pb_{0.11})_{\Sigma 6.81}{}^{X3'}(Bi)_{\Sigma 1.08}{}^{X4}(Ca_{0.93}Ce_{0.07})_{\Sigma 1.00}{}^{Y1}(Mn_{0.47}Mg_{0.24}Fe_{0.19}Cu_{0.10})_{\Sigma 1.00}{}^{Y2}(Al_{3.50}Ti_{0.44}Fe_{0.04}Mg_{0.02})_{\Sigma 4.00}{}^{Y3}(Al_{4.17}Fe_{1.79}Mg_{1.62}Ti_{0.40})_{\Sigma 8.00}{}^{T1}(Al)_{\Sigma 0.11}{}^{Z1}(Si_{1.84}Al_{0.16})_{\Sigma 2.00}{}^{Z2}(Si)_{\Sigma 8.00}{}^{Z3}(Si)_{\Sigma 8.00}O_{68}{}^{O10}(OH)_{2.00}{}^{O11}[(OH)_{7.55}O_{0.45}]_{\Sigma 8.00}$$

The allocation of Pb^{2+} at the X3 site is consistent with the fact that Pb^{2+} is the largest cation detected in this study and the X3-centered polyhedron is the largest one of the present vesuvianite (Table 5). As the observed $^{[8]}$<X3-O> distance (~2.54 Å) is larger than the typical mean distance shown by other vesuvianites with the X3 site occupied solely by Ca (~2.50 Å,

Groat et al. 1992b; Groat and Evans 2012), the accommodation of the large Pb^{2+}-cation at the X3 site seems to be realistic. In addition, observed site-scattering and bond-valence values are not consistent with an occurrence of Pb^{2+} at X1, X2 or X4 sites. The distribution of the atoms over the [5]- and [6]-coordinated sites suggests that: Y1 is populated by cations with formal valence = 2 such as Mn^{2+}; Y2 is dominated by cations with formal valence ≥ 3 such as Al^{3+} and Ti^{4+}; Y3 is populated by cations with mixed formal valence ranging from 2 to 4, although Al^{3+} is the dominant cation. The total OH content was calculated from the charge balance, whereas the anion distributions over the O10 and O11 site were determined by bond valence considerations (see below).

A possible structural formula for our most Bi-rich vesuvianite (analysis 740:X4Core1 in Table 1) may be derived on the basis of the results of the present study and those of Groat and Evans (2012):

$^{X1}(Ca)_{\Sigma 2.00}{}^{X2}(Ca)_{\Sigma 8.00}{}^{X3}(Ca_{4.61}Pb_{0.14})_{\Sigma 4.75}{}^{X3'}(Bi)_{\Sigma 3.19}{}^{X4}(Ca_{0.97}Ce_{0.03})_{\Sigma 1.00}{}^{Y1}(Fe_{0.11}Mg_{0.17}Mn_{0.56}Cu_{0.10}Zn_{0.06})_{\Sigma 1.00}{}^{Y2}(Al_{3.87}Fe_{0.03}Mg_{0.10})_{\Sigma 4.00}{}^{Y3}(Al_{4.64}Fe_{1.41}Mg_{1.84}Ti_{0.11})_{\Sigma 8.00}{}^{T1}(As_{0.28})_{\Sigma 0.28}{}^{Z1}(Si_{1.70}Al_{0.08})_{\Sigma 1.78}{}^{Z2}(Si)_{\Sigma 8.00}{}^{Z3}(Si)_{8.00}O_{68}(OH,O)_{11}$

Bond valences at the O10 and O11 sites

In the vesuvianite structure, the O10 site is bonded to the atoms at the X3 (× 4) and Y1 sites, excluding H. As the present sample shows two distinct X3- and X3'-sites, two site configurations must be taken into account for O10: (X3-X3-X3-X3-Y1) and (X3'-X3'-X3'-X3'-Y1). Such configurations give BVS at O10 equal to 1.09 vu and 0.83 vu, respectively, indicating that the O10 site is occupied completely by (OH).

Excluding H, the O11 site is bonded to the atoms at the X3, Y2 and Y3 sites; when the T1 site is occupied, O11 is also bonded to the atoms at T1, Y2, and Y3 sites. Consequently, for the present sample, three site configurations must be taken into account for O11: (X3-Y2-

Y3), yielding BVS at O11 = 1.12 vu; (X3'-Y2-Y3), yielding BVS at O11 = 1.68 vu; (T1-Y2-Y3), yielding BVS at O11 = 1.91 vu. These values indicate that the O11 site is occupied by both (OH) and O^{2-}. As the amount of Ca^{2+} (plus Pb^{2+}) at X3 is much larger than that of Bi^{3+} at X3' as well as than that of Al^{3+} at T1 (about 6.8 apfu, 1.1 apfu and 0.1 apfu, respectively), the BVS at O11 calculated for the configuration (X3-Y2-Y3) should represent the dominant mean valence at O11: weighted mean value = 1.2 vu. This latter value suggests that the amount of OH at O11 should be much larger than that of O^{2-}.

Hence, combined bond-valence and charge-balance information suggests the following O10 and O11 site populations for the present Bi-rich vesuvianite: $^{O10}(OH)_{2.00}$ and $^{O11}[(OH)_{7.55}O_{0.45}]$.

Bismuthian vesuvianite

The refined unit-cell parameters for our sample with Bi^{3+} ~1.1 apfu [a = 15.7018(6) Å, c = 11.8648(6) Å and V = 2925.2(2) Å^3] are larger than those reported by Goat and Evans (2012) for a sample with Bi^{3+} about 0.4 apfu [a = 15.595(1) Å, c = 11.779(1) Å and V = 2864.7(9) Å^3]. To our knowledge, the cell parameters here refined are the largest ones observed so far for *P4/nnc* vesuvianite. The crystallographic position of Bi^{3+} in our sample and its $^{[8]}$<Bi-O> distance are statistically identical to those refined by Goat and Evans (2012), respectively: 0.9105(1) 0.8343(1) 0.8687(2) and 0.911(1) 0.836(1) 0.868(2); 2.529 Å and ~2.52 Å. Therefore, we can conclude that Bi^{3+} is strongly ordered at the Wyckoff position 16*k* of the vesuvianite structure. This position (X3') is close to the X3 site, and except for Bi no other atoms seem to occupy it.

Provided that Ca is replaced by only Bi at X3 sites four apfu Bi^{3+} (approximately 25 wt% Bi_2O_3) would be required to define a Bi-dominant vesuvianite group mineral species. Although concentrations of Bi^{3+} up to ~3.2 apfu have been detected in vesuvianite crystals

investigated in the present study, the quality of crystals with Bi^{3+}-concentrations significant higher than 1.1 apfu is very poor and they were found to be unsuitable for single-crystal X-ray diffraction studies. This raises questions regarding the stability and borders of flexibility of the vesuvianite structure and whether it can accommodate larger amounts of Bi^{3+} than those recorded in this study. Consequently, the occurrence of a Bi-dominant end-member vesuvianite remains doubtful.

ACKNOWLEDGEMENTS

We thank Hans Harryson for careful microprobe analytical work. Support from the Swedish Research Council (VR) is gratefully acknowledged. We appreciate constructive comments and suggestions on an earlier manuscript version by the two official reviewers Edwin Gnos and Lee Groat. We also want to express our appreciation of the careful manuscript handling by Fernando Colombo (associate editor) and Keith Putirka (editor).

REFERENCES CITED

Allen, F.M. and Burnham, C.W. (1992) A comprehensive structure-model for vesuvianite: Symmetry variations and crystal growth. Canadian Mineralogist, 30, 1-18.

Allen, R.L., Lundström, I., Ripa, M., Simeonov, A., and Christofferson, H. (1996) Facies analysis of a 1.9 Ga, continental margin, back-arc, felsic caldera province with diverse Zn-Pb-Ag-(Cu-Au) sulphide and Fe oxide deposits, Bergslagen region, Sweden. Economic Geology, 91, 979-1008.

Andersson, U.B. (1997) The late Svecofennian, high-grade contact and regional metamorphism in southwestern Bergslagen (central southern Sweden). Geological Survey of Sweden, research report 03-819/93. 29 pp.

Armbruster, T. and Gnos, E. (2000a) *P4/n* and *P4nc* long range ordering in low-temperature vesuvianites. American Mineralogist, 85, 563-569.

Armbruster, T. and Gnos, E. (2000b) Tetrahedral vacancies and cation ordering in low-temperature Mn-bearing vesuvianites: indication of a hydrogarnet-like substitution. American Mineralogist, 85, 570-577.

Armbruster, T., Gnos, E., Dixon, R., Gutzmer, J., Heiny, C., Dobelin, N., and Medenbach, O. (2002) Manganvesuvianite and tweddelite, two new minerals from the Wessels Mine, Kalahari manganese field, South Africa. Mineralogical Magazine, 66, 137-150.

Bosi, F., Balić-Žunić, T., and Surour, A.A. (2010) Crystal structure analysis of four tourmalines from the Cleopatra's Mines (Egypt) and Jabal Zalm (Saudi Arabia), and the role of Al in the tourmaline group. American Mineralogist, 95, 510-518.

Bosi, F., Hålenius, U., and Skogby, H. (2010) Crystal chemistry of the $MgAl_2O_4$-$MgMn_2O_4$-$MnMn_2O_4$ system: Analysis of structural distortion in spinel and hausmannite-type structures. American Mineralogist, 95, 602-607.

Boström, K., Rydell, H., and Joensuu, O. (1979) Långban - an exhalative sedimentary deposit? Economic Geology, 74, 1002-1011.

Britvin, S.N., Antonov, A.A., Krivovichev, S.V., Armbruster, T., Burns, P.C., and Chukanov, N.V. (2003) Fluorvesuvianite, $Ca_{19}(Al,Mg,Fe^{2+})_{13}[SiO_4]_{10}[Si_2O_7]_4O$ $(F,OH)_9$, a new mineral species from Pitkäranta, Karelia, Russia: Description and crystal structure. Canadian Mineralogist, 41, 1371-1380.

Brown, I.D. and Altermatt, D. (1985) Bond-valence parameters obtained from a systematic analysis of the Inorganic Crystal Structure Database. Acta Crystallographica, B41, 244-247.

449 Christy, A. and Gatedal, K. (2005) Extremely Pb-rich rock-forming silicates including a
450 beryllian scapolite and associated minerals in a skarn from Långban, Värmland,
451 Sweden. Mineralogical Magazine, 69, 995-1018.
452 Fitzgerald, S., Rheingold, A.L., and Leavens, P.B. (1986) Crystal structure of a Cu-bearing
453 vesuvianite. American Mineralogist, 71, 1011-1014.
454 Fitzgerald, S., Leavens, P.B., Rheingold, A.L., and Nelen, J.A. (1987) Crystal structure of a
455 REE-bearing vesuvianite from San Benito County, California. American Mineralogist,
456 72, 625-628
457 Flink, G. (1923) Über die Långbansgruben als Mineralvorkommen. Eine vorläufige
458 Orientierung. Zeitschrift für Kristallographie, 58, 356-385.
459 Galuskin, E.V., Galuskina, I.O., Sitarz, M., and Stadnicka, K. (2003) Si-deficient, OH-
460 substituted, boron-bearing vesuvianite from the Wiluy River, Yakutia, Russia. Canadian
461 Mineralogist, 41, 833-842.
462 Galy J., Meunier G., Andersson S. and Åström A. (1975) Stéréochimie des eléments
463 comportant des paires non liées: Ge(II), As(III), Se(IV), Br(V), Sn(II), Sb(III), Te(IV),
464 I(V), Xe(VI) , Tl(I), Pb(II), et Bi(III) (Oxydes, fluorures et oxyfluorures) Jornal of Solid
465 State Chemistry, 13, 142-159.
466 Giacovazzo, C., Monaco, H.L., Artioli, G., Viterbo, D., Ferraris, G., Gilli, G., Zanotti, G., and
467 Catti, M. (2002) Fundamentals of Crystallography, 584 p. Oxford University Press,
468 U.K.
469 Gnos, E. and Armbruster, T. (2006) Relationship among metamorphic grade, vesuvianite "rod
470 polytypism," and vesuvianite composition. American Mineralogist 91, 862-870.
471 Grew, E.S., Yates, M.G., Belakovskiy, D.I., Rouse, R.C., Su, S.-C., and Marquez, N. (1994)
472 Hyalotekite from reedmergnerite-bearing peralkaline pegmatite, Dara-i-Pioz, Tajikistan

and from Mn skarn, Långban, Värmland, Sweden: A new look at an old mineral. Mineralogical Magazine, 58, 285-297.

Groat, L.A. and Evans, R.J. (2012) Crystal chemistry of Bi- and Mn-bearing vesuvianite from Långban, Sweden. American Mineralogist, 97, 1627-1634.

Groat, L.A., Hawthorne, F.C., and Ercit, T.S. (1992a) The chemistry of vesuvianite. Canadian Mineralogist, 30, 19-48.

Groat, L.A., Hawthorne, F.C., and Ercit, T.S. (1992b) The role of fluorine in vesuvianite: A crystal-structure study. Canadian Mineralogist, 30, 1065-1075.

Groat, L.A., Hawthorne, F.C., and Ercit, T.S. (1994a) Excess Y-group cations in the crystal structure of vesuvianite. Canadian Mineralogist, 32, 497-504.

Groat, L.A., Hawthorne, F.C., and Ercit, T.S. (1994b) The incorporation of boron into the vesuvianite structure. Canadian Mineralogist, 32, 505-523.

Groat, L.A., Hawthorne, F.C., Lager, G.A., Schutz, A.J., and Ercit, T.S. (1996) X-ray and neutron crystal-structure refinements of a boron-bearing vesuvianite. Canadian Mineralogist, 34, 1059-1070.

Groat, L.A., Hawthorne, F.C., Ercit, T.S., and Grice, J.D. (1998) Wiluite, $Ca_{19}(Al,Mg,Fe,Ti)_{13}(B,Al,o)_5Si_{18}O_{68}(O,OH)_{10}$, a new mineral species isostructural with vesuvianite, from the Sakha Republic, Russian Federation. Canadian Mineralogist, 36, 1301-1304.

Himmelberg, G.R. and Miller, T.P. (1980) Uranium- and thorium-rich vesuvianite from the Seward Peninsula, Alaska. American Mineralogist, 65, 1020-1025.

Holtstam, D. and Langhof, J. (eds.) (1999) Långban, the mines, their minerals, history and explorers. Raster Förlag, Stockholm. 215 pp.

Holtstam, D. and Mansfeld, J. (2001) Origin of a carbonate-hosted Fe-Mn-(Ba-As-Pb-Sb-W) deposit of Långban-type in central Sweden. Mineralium Deposita, 36, 641-657.

Jonsson, E. (2004) Fissure-hosted mineral formation and metallogenesis in the Långban Fe-Mn-(Ba-As-Pb-Sb…) deposit, Sweden. Meddelanden från Stockholms Universitets Institution för Geologi och Geokemi 318, 110 pp.

Jonsson, E. and Broman, C. (2002) Fluid inclusions in late-stage Pb-Mn-As-Sb mineral assemblages in the Långban deposit, Bergslagen, Sweden. Canadian Mineralogist, 40, 47-65.

Magnusson, N.H. (1930) Långbans malmtrakt. Sveriges Geologiska Undersökning, Ca 23, 1-111.

Moore, P.B. (1970) Mineralogy and chemistry of Långban-type deposits in Bergslagen, Sweden. Mineralogical Record, 1, 154-172.

Pan, Y.M. and Fleet, M.E. (1992) Mineral chemistry and geochemistry of vanadium silicates in the Hemlo gold deposit, Ontario, Canada. Contributions to Mineralogy and Petrology, 109, 511-525.

Pouchou, J.L. and Pichoir, F. (1991) Quantitative analysis of homogeneous or stratified microvolumes applying the model "PAP." In K.F.J. Heinrich and D.E. Newbury, Eds., Electron Probe Quantitation, p. 31-75. Plenum, New York

Shannon, R.D. (1976) Revised effective ionic radii and systematic studies of interatomic distances in halides and chalcogenides. Acta Crystallographica, A32, 751–767.

Sheldrick, G.M. (2008) A short history of SHELX. Acta Crystallographica, A64, 112-122.

Stephens, M. B., Ripa, M., Lundström, I., Persson, L., Bergman, T., Ahl, M., Wahlgren, C.-H., Persson, P.-O., and Wickström, L. (2009) Synthesis of the bedrock geology in the Bergslagen region, Fennoscandian Shield, south-central Sweden. Sveriges Geologiska Undersökning, Ba 58, 1-259.

521 Welin, E. (1992) Isotopic results of the Proterozoic crustal evolution of south-central Sweden;
522 review and conclusions. Geologiska Föreningens i Stockholm Förhandlingar, 114, 299-
523 312.

524

525 TABLES

526

527 TABLE 1. Microprobe analyses of selected crystals of bismuthian vesuvianite from Långban.

528

529 TABLE 2. X-ray diffraction data collection and structural refinement information.

530

531 TABLE 3. Fractional atomic coordinates, equivalent (U_{eq}) or isotropic (U_{iso}*) displacement
532 parameters (Å^2) and mean atomic number (m.a.n.) for bismuthian vesuvianite.

533

534 TABLE 4 **(on deposit).** Anisotropic displacement parameters (Å^2) for bismuthian vesuvianite

535

536 TABLE 5. Selected bond distances (Å) for bismuthian vesuvianite.

537

538 TABLE 6. Bond valence sum (BVS) and mean formal valence (MFV) for bismuthian
539 vesuvianite.

540

541

542 FIGURE CAPTIONS

543

544 FIGURE 1. Back-scattered electron image of crystal 740:X4 displaying a Bi-rich core (white)
545 and a rim characterized by low Bi-concentrations. Numbers indicate Bi concentrations
546 in atoms per formula unit.

547

548 FIGURE 2. Back-scattered electron image (a) and X-ray distribution maps for CaK_α- (b),
549 BiM_α- (c), SiK_α- (d), AlK_α- (e) and FeK_α-radiation (f) of crystal 740:X2. Scale bar
550 equals100 μm.

551

552 FIGURE 3. Bi-concentrations plotted versus the sum of the additional main X-site cations (Ca
553 + Pb + Ce) in the analyzed vesuvianite crystals (open squares). The solid line shows a
554 linear least squares fit ($r^2 = 0.989$) of our data and the broken line indicates the expected
555 relationship for an ideal sum of 19 X cations per formula unit. The two filled triangles
556 in the lower right-hand corner of the figure show for comparison the corresponding
557 values reported by Groat and Evans (2012).

558

559 FIGURE 4. Projection along the **c**-direction showing the clustering of X3- (Ca), X3´-sites (Bi)
560 and their adjacent T- and Y-sites (A) and a close-up of this projection highlighting the
561 coordination at adjacent occupied X3- and X3´-sites. The O10 site is fully occupied by
562 OH and O11 is partially OH-occupied, while the remaining oxygen positions are not
563 hydrogen related.

564

TABLE 1. Microprobe analyses of selected crystals of bismuthian vesuvianite from Långban

Sample	740:X1Core	740:X1SREF*	740:X2Core1	740:X2Core2	740:X2Core3	740:X2Rim	740:X3Core	740:X4Core1	740:X4Core2	740:X4Rim
SiO_2 wt.%	29.39	32.89	29.16	28.83	31.83	35.92	30.92	29.18	30.12	35.27
As_2O_5	1.41	0.00	1.24	0.87	0.90	0.00	0.60	0.87	0.24	0.92
Al_2O_3	10.64	12.40	10.88	10.28	11.88	16.96	10.47	12.01	11.05	16.24
TiO_2	1.28	2.08	1.24	2.28	2.16	0.63	1.51	0.25	1.55	0.98
MgO	2.66	2.33	2.48	2.02	2.56	2.06	2.86	2.33	2.77	2.19
MnO	1.33	1.15	1.25	1.17	0.90	0.57	1.41	1.21	1.26	0.55
FeO	5.64	4.95	4.87	4.92	4.69	2.46	5.30	3.39	5.14	3.27
CuO	0.15	0.29	0.23	0.13	0.24	0.77	0.32	0.22	0.25	0.81
ZnO	0.06	0.01	0.00	0.15	0.00	0.08	0.04	0.14	0.10	0.00
CaO	26.01	30.33	25.05	23.41	29.29	35.27	27.17	23.98	26.37	35.36
PbO	0.88	0.77	0.72	5.28	0.86	0.40	0.82	0.85	0.72	0.50
Ce_2O_3	1.02	0.33	0.90	1.05	0.45	0.01	1.73	0.15	0.82	0.00
Sb_2O_3	0.00	0.00	0.01	1.03	0.06	0.00	0.03	0.00	0.00	0.00
Bi_2O_3	15.34	7.69	17.52	14.35	9.62	0.58	12.15	20.42	16.07	0.76
SUM	95.81	95.20	95.54	95.77	95.43	95.62	95.32	95.00	96.46	96.88
Atoms per formula unit on the basis of 50 cations										
Si	17.199	17.844	17.374	17.591	17.601	17.882	17.687	17.699	17.401	17.529
As	0.431	0.000	0.385	0.276	0.261	0.000	0.179	0.276	0.072	0.240
Al	0.370	0.156	0.241	0.133	0.138	0.118	0.134	0.025	0.527	0.231
Sum [4]-coordinated	*18.000*	18.000	*18.000*	*18.000*	*18.000*	*18.000*	*18.000*	*18.000*	*18.000*	*18.000*
Ti	0.563	0.847	0.555	1.046	0.898	0.235	0.649	0.114	0.673	0.366
Al	6.966	7.771	7.399	7.260	7.603	9.834	6.927	8.560	6.997	9.283
Mg	2.323	1.880	2.200	1.837	2.107	1.532	2.439	2.107	2.386	1.622
Mn	0.591	0.476	0.565	0.546	0.377	0.216	0.614	0.559	0.554	0.210
Fe	2.482	2.019	2.184	2.261	1.951	0.921	2.281	1.547	2.235	1.223
Cu	0.068	0.118	0.102	0.058	0.100	0.290	0.138	0.101	0.109	0.304
Zn	0.027	0.003	0.000	0.069	0.000	0.031	0.015	0.063	0.043	0.000
Sum [5]- and [6]-coordinated	*13.020*	13.114	*13.005*	*13.077*	*13.036*	*13.059*	*13.063*	*13.051*	*12.997*	*13.008*
Ca	16.306	17.632	15.988	15.304	17.357	18.810	16.649	15.583	16.323	18.827
Pb	0.139	0.112	0.115	0.868	0.129	0.054	0.127	0.139	0.112	0.067
Ce	0.218	0.065	0.197	0.233	0.091	0.002	0.362	0.033	0.173	0.000
Sb	0.000	0.000	0.003	0.258	0.014	0.000	0.007	0.000	0.000	0.000
Bi	2.315	1.076	2.692	2.258	1.373	0.074	1.792	3.195	2.394	0.098
Sum [7]- to [9]-coordinated	*18.978*	18.885	*18.995*	*18.921*	*18.964*	*18.940*	*18.937*	*18.950*	*19.002*	*18.992*

*Crystal fragment used for structure refinement

TABLE 2. X-ray diffraction data collection and structural refinement information

	Crystal data
Space group	*P4/nnc*
Z	2
a (Å)	15.7018(6)
c (Å)	11.8648(6)
V (Å^3)	2925.2(2)
Crystal sizes (mm)	$0.12 \times 0.10 \times 0.02$
	Data Collection and refinement
Radiation, Mo-*K*α (Å)	0.71073
Temperature (K)	298(2)
Total number of frames	3304
Range for data collection, 2θ (°)	4 - 61
Reciprocal space range *hkl*	$-22 \leq h \leq 22$
	$-21 \leq k \leq 21$
	$-16 \leq l \leq 16$
Set of read reflections	29575
Unique reflections	2248
Absorption correction method	Multi-scan
Refinement method	Full-matrix least-squares on F^2
R_{int}	0.782
Completeness	0.995
Redundancy	12
Extinction coefficient	0.0003(1)
w*R*2	0.1373
*R*1 all data	0.0880
*R*1 for $I > 2\sigma_I$	0.0493
GooF	1.044
Diff. Peaks ($\pm e^-$/Å^3)	1.68; –1.32

Notes: $R_{int.}$ = merging residual value; *R*1 = discrepancy index, calculated from *F*-data; *wR*2 = weighted discrepancy index, calculated from F^2-data; GooF = goodness of fit; Diff. Peaks = maximum and minimum residual electron density.

TABLE 3. Fractional atomic coordinates, equivalent (U_{eq}) or isotropic (U_{iso}*) displacement parameters (Å^2) and mean atomic number (m.a.n.) for Bi-rich vesuvianite

Site	*x*	*y*	*z*	$U_{eq,}/U_{iso}$*	m.a.n.
X1	3/4	1/4	1/4	0.0169(4)	20
X2	-0.18937(6)	0.04448(7)	0.37940(8)	0.0142(2)	20
X3	-0.10225(12)	-0.18232(12)	0.89613(17)	0.0239(4)*	16.2(1)
X3'(≡Bi)	0.91052(14)	0.83432(14)	0.86868(19)	0.0204(6)*	10.3(1)
X4	3/4	3/4	0.1416(4)	0.0291(16)	11.6(1)
Y1	3/4	3/4	0.0483(5)	0.0267(17)	10.9(3)
Y2	0	0	0	0.0128(6)	13.5(1)
Y3	-0.11248(8)	0.12049(8)	0.12697(10)	0.0124(4)	15.0(1)
T1	0.0566(8)	0.0566(8)	1/4	0.012(4)*	1.43(2)
Z1	3/4	1/4	0	0.0100(8)	13.1(2)
Z2	-0.17996(9)	0.04190(9)	0.87164(11)	0.0110(5)	13.0(1)
Z3	-0.08294(9)	-0.15023(9)	0.36360(11)	0.0139(3)	14
O1	-0.2204(2)	0.1730(2)	0.0852(3)	0.0171(8)	8
O2	-0.1180(2)	0.1602(2)	0.2801(3)	0.0190(8)	8
O4	-0.0618(2)	0.1057(2)	0.4692(3)	0.0156(7)	8
O3	-0.0470(2)	0.2236(2)	0.0757(3)	0.0164(7)	8
O5	-0.1717(2)	0.0135(2)	0.1782(3)	0.0206(8)	8
O6	0.8799(3)	-0.2742(3)	0.0583(3)	0.0270(9)	8
O7	0.0543(3)	0.1712(3)	0.3197(3)	0.0272(9)	8
O8	-0.0604(2)	-0.0910(2)	0.0680(3)	0.0176(8)	8
O9	-0.1440(2)	-0.1440(2)	1/4	0.0205(11)	8
O10	3/4	3/4	0.8658(10)	0.051(3)	8
O11	-0.0036(2)	0.0620(2)	0.1361(3)	0.0167(7)	8

.

TABLE 4 (on deposit). Anisotropic displacement parameters ($Å^2$) for bismuthian vesuvianite

Site	U^{11}	U^{22}	U^{33}	U^{23}	U^{13}	U^{12}
Z1	0.0120(10)	0.0120(10)	0.0059(13)	0	0	0
Z2	0.0104(7)	0.0157(8)	0.0070(7)	0.0023(5)	-0.0010(5)	0.0004(5)
Z3	0.0195(7)	0.0137(6)	0.0086(6)	-0.0011(5)	0.0003(5)	0.0025(5)
X1	0.0269(11)	0.0150(10)	0.0088(8)	0	0	0
X2	0.0140(5)	0.0182(5)	0.0104(5)	-0.0005(4)	-0.0016(4)	0.0008(4)
X4	0.0197(16)	0.0197(16)	0.048(4)	0	0	0
Y1	0.0142(16)	0.0142(16)	0.052(4)	0	0	0
Y2	0.0133(10)	0.0128(10)	0.0124(9)	0.0017(8)	0.0019(8)	0.0004(8)
Y3	0.0142(7)	0.0139(7)	0.0092(6)	0.0003(5)	0.0011(5)	0.0007(4)
O1	0.0236(19)	0.0167(17)	0.0108(16)	0.0006(14)	0.0011(15)	-0.0012(14)
O2	0.0226(19)	0.0201(19)	0.0142(17)	0.0020(15)	-0.0041(15)	-0.0010(15)
O4	0.0198(19)	0.0175(18)	0.0096(17)	0.0003(14)	-0.0028(13)	-0.0014(14)
O3	0.0222(19)	0.0166(18)	0.0103(16)	-0.0011(14)	-0.0003(14)	0.0028(14)
O5	0.0185(19)	0.027(2)	0.0160(18)	-0.0040(16)	0.0019(15)	0.0063(16)
O6	0.039(2)	0.025(2)	0.0170(18)	0.0041(16)	0.0045(18)	0.0080(17)
O7	0.025(2)	0.037(2)	0.020(2)	0.0064(18)	0.0010(17)	0.0085(18)
O8	0.0167(17)	0.0189(18)	0.0171(18)	0.0020(14)	0.0066(14)	0.0023(15)
O9	0.0272(17)	0.0272(17)	0.007(2)	0.0011(16)	-0.0011(16)	-0.004(2)
O10	0.034(3)	0.034(3)	0.085(9)	0	0	0
O11	0.0156(17)	0.0191(18)	0.0155(17)	-0.0036(14)	-0.0020(14)	-0.0016(15)

.

TABLE 5. Selected bond distances (Å) for bismuthian vesuvianite

distance		distance		distance	
X1-O1 (x4)	2.345(4)	X3'-O11	2.188(4)	Y3-O2	1.922(4)
X1-O2 (x4)	2.532(4)	X3'-O7	2.245(4)	Y3-O11	1.944(4)
[8]<X1-O>	**2.439**	X3'-O7	2.304(5)	Y3-O1	1.948(4)
		X3'-O3	2.419(4)	Y3-O3	2.012(4)
X2-O5	2.337(4)	X3'-O8	2.679(4)	Y3-O5	2.014(4)
X2-O8	2.342(4)	X3'-O7	2.684(5)	Y3-O4	2.089(4)
X2-O3	2.390(4)	X3'-O10	2.847(2)	**[6]<Y3-O>**	**1.988**
X2-O2	2.438(4)	X3'-O6	2.863(5)		
X2-O5	2.451(4)	**[8]<X3'-O>**	**2.529**	Z1-O1 (x4)	1.643(4)
X2-O4	2.464(4)			**[4]<Z1-O>**	**1.643**
X2-O1	2.502(4)	X4-O6 (x4)	2.297(5)		
X2-O6	3.000(4)	X4-O9 (x4)	2.683(5)	Z2-O7	1.637(4)
[8]<X2-O>	**2.491**	**[8]<X4-O>**	**2.490**	Z2-O3	1.641(4)
				Z2-O2	1.645(4)
X3-O6	2.420(4)	Y1-O6 (x4)	2.077(4)	Z2-O4	1.673(4)
X3-O3	2.454(4)	Y1-O10	2.165(14)	**[4]<Z2-O>**	**1.649**
X3-O7	2.457(4)	**[5]<Y1-O>**	**2.095**		
X3-O11	2.544(4)			Z3-O6	1.615(4)
X3-O10	2.577(2)	Y2-O11 (x2)	1.887(3)	Z3-O5	1.629(4)
X3-O8	2.578(4)	Y2-O8 (x2)	1.895(3)	Z3-O8	1.632(4)
X3-O7	2.585(5)	Y2-O4 (x2)	1.956(3)	Z3-O9	1.657(2)
X3-O7	2.674(5)	**[6]<Y2-O>**	**1.912**	**[4]<Z3-O>**	**1.634**
[8]<X3-O>	**2.536**				
X3-O6	2.902(4)			T1-O11 (x2)	1.651(8)
[9]<X3-O>	**2.577**			T1-O7 (x2)	1.980(12)
				[4]<T1-O>	**1.816**

TABLE 6. Bond valence sum (BVS) and mean formal valence (MFV) for Bi-rich vesuvianite

Site	BVS/MFV	Site	BVS/MFV	Site	BVS/MFV	Site	BVS/MFV
X1	2.31/2.00	**X2**	2.16/2.00	**X3**	1.85/2.00	**X3'**	3.09/3.00
X4	2.22/2.07	**Y1**	1.95/2.00	**Y2**	3.13/3.10	**Y3**	2.68/2.62
T1	2.82/3.00	**Z1**	3.80/3.92	**Z2**	3.74/4.00	**Z3**	3.90/4.00

Notes: X3' ≡ Bi; MFV derived from the structural formula

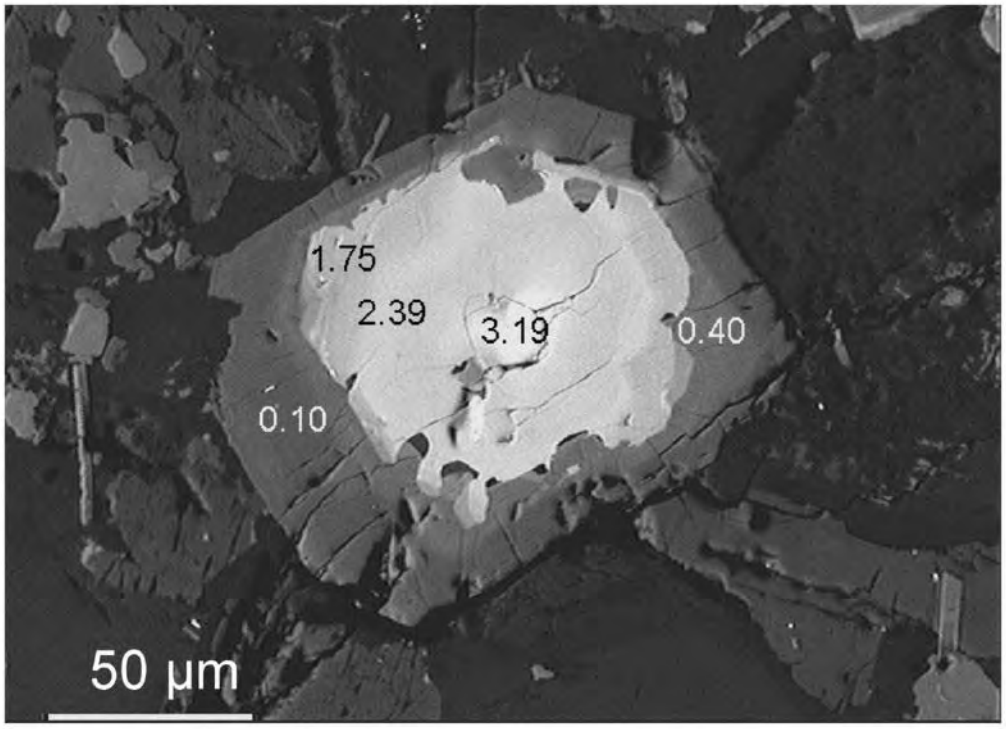

Figure1

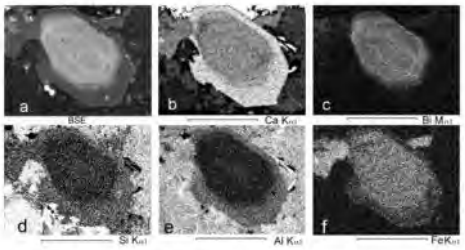

Figure 2

Figure 3

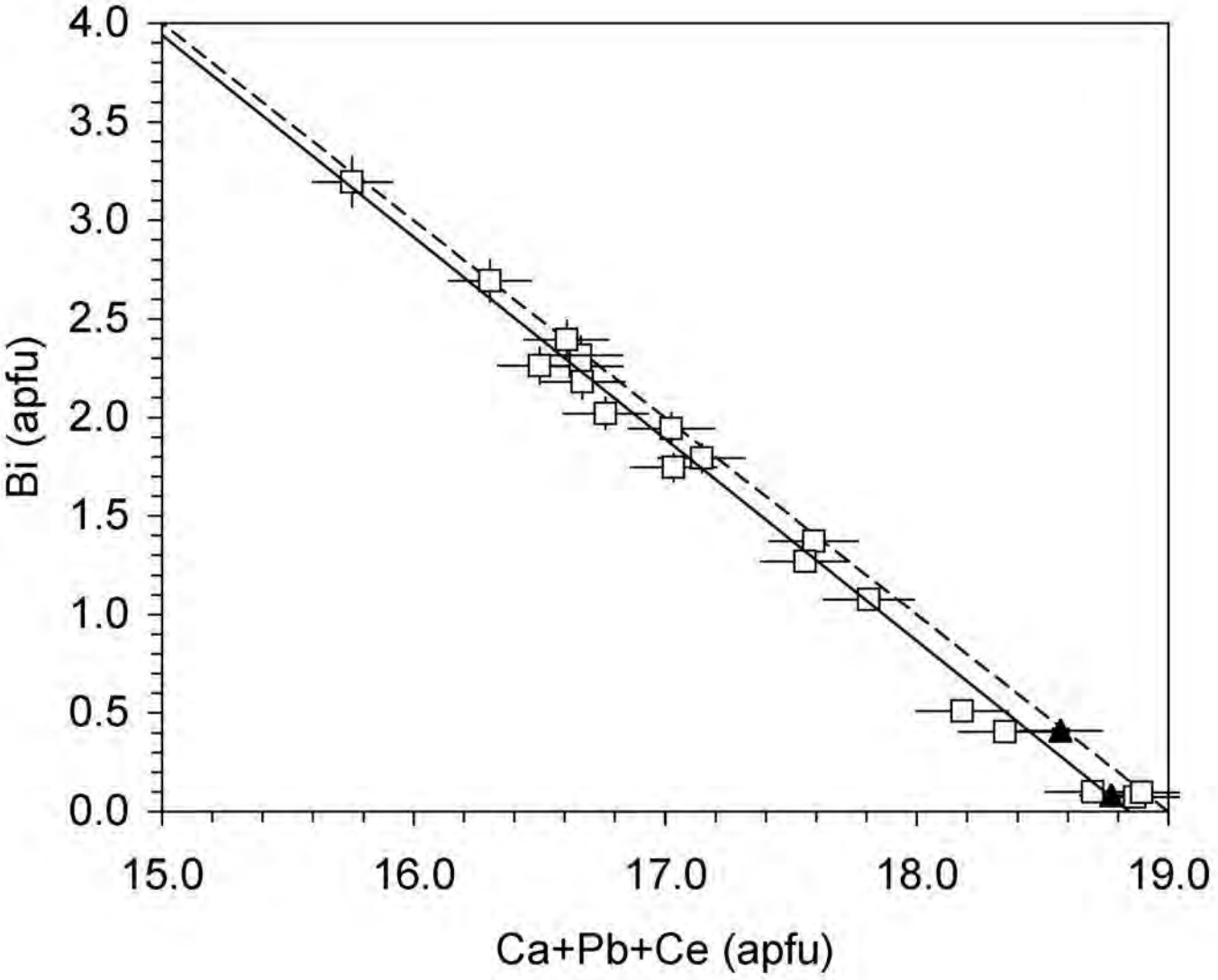

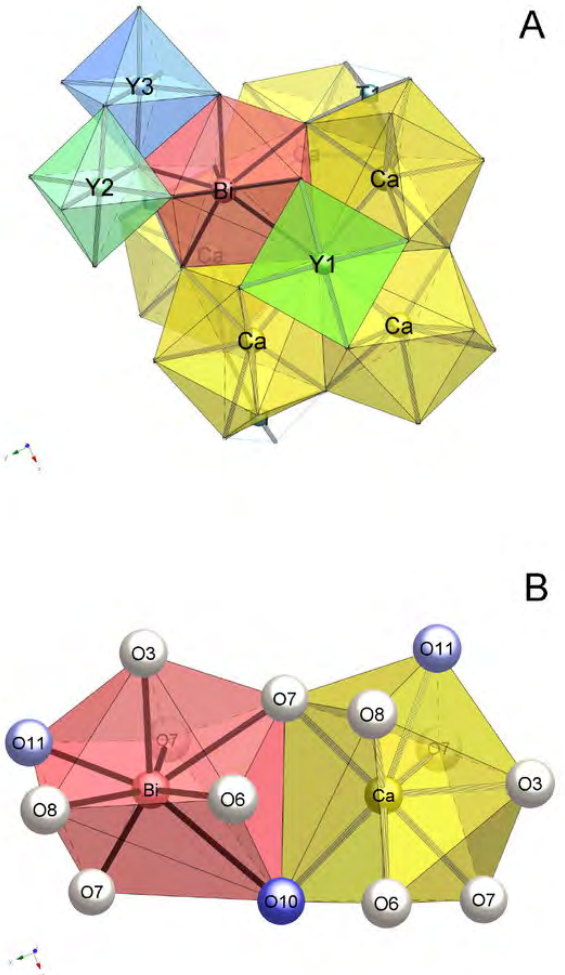

Figure 4